# Adaptive Direction of Arrival Estimation and Beamforming Algorithms for Future Networks and Advancements

ADAM MOHAMED AHMED ABDO[1,2], MOHAMED HUSSIEN MOHAMED NERMA[3,4], AAMER MOHAMED HUROON MOHAMED[2]

[1]Departmenet of Electrical Engineering,
Gulf of Sidra University,
College of Engineering Science, Sirte,
LIBYA

[2]Department of Electrical and Electronics Engineering,
University of Nyala,
Faculty of Engineering Science, Nyala,
SUDAN

[3]Department of Computer Engineering,
University of Tabuk,
Faculty of Computer and Information Technology, Tabuk, 71491,
SAUDI ARABIA

[4]Department of Electronic Engineering,
Sudan University of Science and Technology,
Faculty of Engineering, Khartoum,
SUDAN

*Abstract:* - Multiuser Multiple Input Multiple Output (MU-MIMO) wireless communication systems significantly enhance mobile cellular networks by employing Direction of Arrival (DOA) algorithms and beamforming (BF) techniques. These technologies enable the prediction of sidelobe signal directions, allowing for redirection toward specific desired targets. This research presents various adaptive DOA algorithms designed to improve wireless network performance. The study thoroughly examines DOA algorithms, including Multi-Signal Classification (MUSIC), Minimum Norm (Min-Norm), Minimum Variance Distortionless Response (MVDR), and Bartlett algorithms, comparing them based on angle estimation and peak power spectrum. The paper also discusses the concept of separating incoming signals into the Signals of Interest (SOI) and Signals Not of Interest (SNOI). Additionally, several BF algorithms, such as Least Mean Square (LMS), Recursive Least Square (RLS), and Constant Modulus Algorithm (CMA), are explored and evaluated. The research assesses the impact of BF algorithms on Bit Error Rate (BER) with varying numbers of antenna elements at the base station (BS). Simulation results indicate that while the algorithms demonstrate similar capabilities for interference cancellation, they differ in peak power values and beam widths. Furthermore, the accuracy of angle scanning and interference reveals that the algorithms have unique effects on directivity and gain, with the RLS algorithm showing slight improvements over the SMI and CMA algorithms. The findings highlight that the selection of beamforming algorithms, along with the number of antenna elements, significantly affects BER performance.

*Key-Words:* - Adaptive BF, DOA, Power Spectrum, Amplitude Radiation, BER, SOI, mm-wave communications, and MU-MIMO.

Received: May 19, 2024. Revised: November 11, 2024. Accepted: December 13, 2024. Published: February 4, 2025.

## 1 Introduction

Beamforming (BF) techniques are central to wireless cellular communication applications, including cellular phone systems, unidirectional radio and TV broadcasting, as well as satellite and radar communications, [1], [2]. In wireless communications, network capacity is primarily limited by user interference both within the same cell and in neighboring cells. BF techniques enhance and direct incoming signals toward the receiver (Rx), acting as a signal manipulation method to filter desired signals that are affected by unwanted interference, such as co-channel interference (CCI) and inter-symbol interference (ISI), [2], [3].

There are two main classes of antenna array signal processing. The first class consists of BF algorithms, including Least Mean Square (LMS), Recursive Least Square (RLS), and Constant Modulus Algorithm (CMA), which have been extensively discussed in prior research. The second class includes Direction of Arrival (DOA) estimation algorithms, such as Multiple Signal Classification (MUSIC), Minimum Variance Distortionless Response (MVDR), and Bartlett algorithms, [4], [5], [6]. The key difference between these categories is that the first class focuses the array signal toward a specific angle in the main beam direction [7], while the second class ensures the accurate arrival of the strongest signal at the correct angle when a fixed base station (BS) communicates with a mobile station (MS) in motion.

DOA estimation is crucial in modern signal processing, especially with the growing demand for wireless cellular communication services. Recent studies have shown that the traditional MUSIC algorithm has difficulties in accurately estimating coherent signals, leading to significant discrepancies between estimated and actual data, [8]. Researchers are actively exploring DOA estimation algorithms for coherent signals and have compared the performance of MUSIC and MVDR against traditional BF algorithms [9], as well as conducting comparative analyses of various DOA algorithms, [10]. However, these studies often involve a limited number of antenna elements within a uniform linear array (ULA) system.

Balancing the increasing demands for data transmission with limited network resources presents a significant challenge. Mobile network managers continually optimize RF resources to address rising data communication requests using BF techniques. Numerous studies have investigated new algorithms for BF processes, such as a study on the RLS BF algorithm that established a new energy model based on the signal-to-interference plus noise ratio (SINR), as well as the distance between the BS and MS and the beam width angle.

This article explores various DOA algorithms with a focus on directing signal vectors, emphasizing the number of antenna elements, that can reach up to 128 in a multiuser massive Multiple Input Multiple Output (MU-MIMO) system. This research has potential applications in future big data and Internet of Things (IoT) scenarios. Additionally, it introduces a novel approach to investigating adaptive BF algorithms, presenting analytical results on steering beams toward Signal of Interest (SOI) and Signal Not of Interest (SNOI) directions. The study also conducts an in-depth analysis of LMS, RLS, and CMA beamforming within the MU-MIMO mm-wave signal band operating at 10 GHz. It evaluates the impact of BF implementation on Bit Error Rate (BER) regarding data accuracy and correctness, providing BER results both with and without the application of BF algorithms.

## 2 System Model

The antenna array structure can be utilized to classify the system model. In a smart array antenna system, various configurations of antenna elements are present on both transceiver sides, with the most common types being the Uniform Linear Array (ULA) and the Uniform Planar Array (UPA). These array sensor elements can be distributed either uniformly or non-uniformly. In a ULA, the Direction of Arrival (DOA) of the signal can be detected and estimated in only one dimension (1D). In contrast, a UPA allows for detection and estimation in two dimensions (2D). This means that, with a UPA, it is possible to determine the location of the signal source in both elevation and azimuth angles. This paper focuses on the basic Uniform Linear Array antenna, [11].

As shown in Figure 1 (Appendix), this paper presents a schematic diagram illustrating the proposed DOA algorithms. The diagram highlights the features of a linear array antenna at the cellular base station (BS), operating at a carrier frequency within the mm-wave band. It is assumed that the array consists of M antenna elements, which receive P signals from various directions. Each antenna element experiences zero-mean Gaussian noise with a normal distribution. Therefore, the output signal y(t)y(t)y(t) generated from all signal sources can be expressed as follows, [2]:

$$y[\mathrm{t}] = \sum_{k=1}^{M} w_k x_k[\mathrm{t}] \tag{1}$$

where $\mathbf{x}(\mathrm{t}) = \mathbf{A}(\theta)\mathrm{s}(\mathrm{t}) + \mathbf{N}(\mathrm{t})$. The received array sensor data $\mathbf{X}(\mathrm{t})$ is $\mathbf{x}(\mathrm{t}) = \left[x_1(\mathrm{t}), x_2(\mathrm{t}), ..., x_M(\mathrm{t})\right]^T$, the constructed array manifold matrix $\mathbf{A}(\theta)$ is $\mathbf{A}(\theta) = \left[\mathbf{a}(\theta_1), \mathbf{a}(\theta_2), ..., \mathbf{a}(\theta_M)\right]$, the incoming signal vector $\mathbf{S}(\mathrm{t})$ is $\mathbf{s}(\mathrm{t}) = \left[s_1(\mathrm{t}), s_2(\mathrm{t}), ..., s_P(\mathrm{t})\right]^T$, and the modeled sensor noise vector $\mathbf{N}(t)$ is $\mathbf{N}(t) = [n_1(t), n_2(t), ..., n_M(t)]^T$. Then, the steering vector "direction-finding vector" can be written as [9], [10]:

$$\mathbf{a}(\theta_i) = \left[1, e^{\frac{j2\pi d}{\lambda}\sin(\theta_i)}, ..., e^{\frac{j2\pi d(M-1)}{\lambda}\sin(\theta_i)}\right]^T \quad (2)$$

where $d$, $\lambda$, and $\theta_i$ are the spacing between array-antenna elements, the wavelength of the signal, and the angle of arrival (AOA) of $i^{th}$ the signal source, respectively. Each user or MS is supposed to have a channel vector $\mathbf{h}_u$ that is constructed based on a given arriving angle, thus $\mathbf{h}_u = \mathbf{a}(\theta_i) \in C^{M\times 1}$ is $M \times 1$ user channel vector. The antenna weight vector $\mathbf{w}$ of the uniform linear array antenna can be obtained from the normalized version of the signal steering vector $\mathbf{a}(\theta)$ by the number of antenna elements factor $M$ [12], [13] as.

$$\mathbf{w}_u = \mathbf{w}_u(\theta) = \frac{1}{M}\left[1, e^{\frac{j2\pi d}{\lambda}\sin(\theta_i)}, ..., e^{\frac{j2\pi d(M-1)}{\lambda}\sin(\theta_i)}\right]^T \quad (3)$$

Subsequently, $M \times M$ channel correlation matrix for each user can be described as follows, [11]:

$$\mathbf{R}_u = \mathrm{E}\left\{\mathbf{h}_u \mathbf{h}_u^{\mathrm{H}}\right\} \quad (4)$$

The precise channel covariance matrix $\mathbf{R}$ is not directly accessible and can be estimated from the vector of received signal data, approximating it as:

$$\hat{\mathbf{R}}_{xx} = \frac{1}{K}\sum_{k=1}^{K} \mathbf{x}\mathbf{x}^H \quad (5)$$

The antenna weight vector is generated by normalizing the steering array response vector. Consequently, the resulting beamforming technique is regarded as traditional, resembling the well-established classical beamforming approach, [14].

# 3 The Direction of Arrival Algorithms

This section provides a detailed overview of various types of Direction of Arrival (DOA) estimation algorithms used in wireless cellular networks. DOA estimation primarily focuses on beamforming techniques that scan all potential arrival angles of incoming signals. Typically, the beamforming scanning angles are expected to range from -90° to +90°. Assuming there are no signals (a null signal) at the back lobe of the antenna, the scanning direction encompasses 180 degrees, which is opposite to the main direction. Therefore, the initial output signal in Equation (1) can be reformulated as follows:

$$y(t) = \mathbf{w}^H x(t) \quad (6)$$

The cumulative received power from the Uniform Linear Array (ULA) elements with NNN signal sources can be expressed as:

$$\begin{aligned} P(\mathrm{w}) &= \frac{1}{N}\sum_{n=1}^{N}\left|y(t_n)\right|^2 \\ &= \frac{1}{N}\sum_{n=1}^{N}\mathbf{w}^H \mathbf{x}(t_n)\mathbf{x}^H(t_n)\mathbf{w} \end{aligned} \quad (7)$$

Using the covariance matrix given in Equation (5), the overall weighted signal power can be restated as:

$$P(\mathrm{w}) = \mathbf{w}^H \hat{\mathbf{R}}_{xx}\mathbf{w} \quad (8)$$

## 3.1 Bartlett Direction of Arrival Algorithm

This subsection presents a mathematical model for the Bartlett DOA algorithm. It includes the computation of signal steering vectors and total received power. The average periodogram algorithm, known as the Bartlett method, is a well-known DOA algorithm in cellular communication. In this type of DOA beamforming structure, the normalized received weight vector is given by:

$$\mathbf{w}_{Bart} = \frac{\mathbf{a}(\theta)}{\sqrt{\mathbf{a}^H(\theta)\mathbf{a}(\theta)}} \quad (9)$$

The power spectrum of the Bartlett method is given by:

$$P_{Bart}(\theta) = \frac{\mathbf{a}^H(\theta)\hat{\mathbf{R}}_{xx}\mathbf{a}(\theta)}{\mathbf{a}^H(\theta)\mathbf{a}(\theta)} \quad (10)$$

The Bartlett technique's beamforming weight vector is considered a spatial filter that aligns with the incoming data signal. Additionally, the Uniform Linear Array antenna compensates for the delays introduced by multipath propagation during signal reception.

## 3.2 Minimum Variance Distortionless Response

A refined version of the Bartlett DOA algorithm is known as the Capon beamforming or "Minimum Variance Distortionless Response" (MVDR) technique. This approach addresses the limitation of the Bartlett method, which has difficulty distinguishing between signal sources that are close together within the beam's width. To overcome this issue, a maximum likelihood method is introduced for MVDR, aiming to maximize the Signal-to-

Interference-plus-Noise Ratio (SINR). Consequently, the resulting weight vector for the Uniform Linear Array (ULA) antenna using the Capon technique is presented as shown in Equation (11):

$$\mathbf{w}_{Capon} = \frac{\hat{\mathbf{R}}_{xx}^{-1}\mathbf{a}(\theta)}{\mathbf{a}^H(\theta)\hat{\mathbf{R}}_{xx}^{-1}\mathbf{a}(\theta)} \tag{11}$$

By substituting the estimated weight vector into the power spectrum formula outlined in Equation (8), the power spectrum received by the array antenna can be expressed as:

$$P(\theta) = \left[\frac{\hat{\mathbf{R}}_{xx}^{-1}\mathbf{a}(\theta)}{\mathbf{a}^H(\theta)\hat{\mathbf{R}}_{xx}^{-1}\mathbf{a}(\theta)}\right]^H \hat{\mathbf{R}}_{xx}\left[\frac{\hat{\mathbf{R}}_{xx}^{-1}\mathbf{a}(\theta)}{\mathbf{a}^H(\theta)\hat{\mathbf{R}}_{xx}^{-1}\mathbf{a}(\theta)}\right] \tag{12}$$

By deriving the formula in Equation (12), we obtain the following expression:

$$P(\theta) = \frac{1}{\mathbf{a}^H(\theta)\hat{\mathbf{R}}_{xx}^{-1}\mathbf{a}(\theta)} \tag{13}$$

## 3.3 Multi Signal Classification

This section focuses on the MUSIC algorithm, a well-known beamforming (BF) technique for Direction of Arrival (DOA) estimation that is extensively utilized in signal processing to determine and monitor incoming signal frequencies. The MUSIC beamformer relies on spectral estimation by exploiting the orthogonality between data signals and noise subspaces. Moreover, the MUSIC technique can identify the DOAs of multiple incoming signal sources, making it a highly spatially efficient algorithm that achieves high accuracy with a minimal number of antenna elements compared to other DOA techniques, [10], [15].

The concept behind the MUSIC scheme involves decomposing the covariance matrix of received signal data through matrix operations to extract orthogonal signal and noise subspaces. The orthogonality between these subspaces is then used to generate the spatial spectrum and estimate the arrival angles of the signals, [15]. In the MUSIC DOA estimation technique, the arrival angles of the received signal or autocorrelation matrix can be estimated using the eigen-space method. This eigen-space technique assumes that the incoming received signal *x(n)* consists of *P* complex exponential signals with additive white Gaussian noise, resulting in an $M \times M$ autocorrelation matrix as outlined in Equation (5), [16].

The principle of the MUSIC scheme based on matrix decomposition can be explained by the following theorem:

***Theorem****: assume a matrix* $\mathbf{A} \in R^{m\times n}$ *with rank* $r \in [0, \min(m,n)]$ *the SVD of* $\mathbf{A}$ *is a decomposition of form* $\mathbf{A} = \mathbf{U}\sum\mathbf{V}^T$, *with an orthogonal matrices* $\mathbf{U} = (u_1, u_2, ..., u_m) \in R^{m\times m}$ *and* $\mathbf{V} = (v_1, v_2, ..., v_n) \in R^{n\times n}$, *while* $\sum$ *is an* $m\times n$ *matrix with* $\sum_{ii} = \sigma_i \geq 0$ *and* $\sum_{ij} = 0,\ i \neq j$

which is uniquely determined for the matrix $\mathbf{A}$. Based on the theorem above and the data model described in Section 2, the MUSIC scheme comprises signal and noise subspaces, resulting from the decomposition process into two orthogonal subspaces $\mathbf{U}_S$ and $\mathbf{U}_N$. The matrix $\boldsymbol{U}$ contains the largest eigenvalues, which correspond to the desired signal sources, while the smallest eigenvalues correspond to the noise signals. Consequently, the DOA angle estimation process can be performed by selecting the smallest eigenvalues, utilizing the noise subspace for DOA angle estimation, [17], [18].

Despite the independence of the received data and noise signals, the resulting cross-correlation matrix matrix $\hat{\mathbf{R}}_{xx}$ obtained in Equation (5) can be decomposed into two submatrices.

$$\begin{aligned}\hat{\mathbf{R}}_{xx} &= \mathbf{U}\Sigma\mathbf{U}^H \\ &= [\mathbf{U}_S, \mathbf{U}_N]\Sigma[\mathbf{U}_S, \mathbf{U}_N]^H \\ &= \mathbf{U}_S\Sigma_S\mathbf{U}_S^H + \mathbf{U}_N\Sigma_N\mathbf{U}_N^H\end{aligned} \tag{14}$$

where $\mathbf{U}_S$ represents the signal subspace, and $\mathbf{U}_N$ represents the noise subspace. While it is assumed that the signal and noise subspaces are orthogonal, achieving this ideal condition in practice can be difficult. Thus, using estimated values becomes essential. Consequently, the DOA angles estimated for the MUSIC technique can be expressed as follows:

$$\theta_{MUSIC} = \arg\min\left[\mathbf{a}^H(\theta)\hat{\mathbf{U}}_N\hat{\mathbf{U}}_N^H\mathbf{a}(\theta)\right] \tag{15}$$

Thus, the power spectrum of the signal calculated using the MUSIC method can be expressed as follows:

$$P_{MUSIC} = \frac{1}{\mathbf{a}^H(\theta)\hat{\mathbf{U}}_N\hat{\mathbf{U}}_N^H\mathbf{a}(\theta)} \tag{16}$$

After performing a peak search within the MUSIC power algorithm and identifying the maximum power values at specific positions, the corresponding angles determine the Direction of Arrival (DOA) angles.

### 3.4 Minimum Norm

The Minimum Norm (Min-Norm) algorithm is acknowledged as a high-resolution technique for angle estimation, similar to the MUSIC algorithm in addressing DOA estimation problems. The Minimum Norm method can be better understood through the following statement. Let us consider the following subspace theorem:

***Theorem***: Assume $\mathbf{V} \in R^n$ is not an empty matrix, which is a collection of vectors, and the matrix $\mathbf{V}$ is called subspace if $a$ and $b$ are scalars and the vectors $\vec{u}$ and $\vec{v}$ are in $\mathbf{V}$, then, the combination of $a\vec{u}+b\vec{v}$ is in $\mathbf{V}$.

Thus, in Minimum Norm DOA estimation, the standard basis subspace is defined according to the following definition:

*Definition:*

Let $\vec{e}$ be a vector in $R^n$ which has a unity entity in the $i^{th}$ entry and all other entities are zeros, the $i^{th}$ column of the identity matrix. Then the formulation $\left\{\vec{e}_1, \vec{e}_2, ..., \vec{e}_n\right\}$ is the basis for $R^n$ and it is called the standard basis of $R^n$. Similarly, the Minimum Norm vector is defined by a standard basis that is optimal for estimating DOA angles based on the noise subspace. Therefore, the $M \times 1$ estimated vector can be represented as shown in Equation (17). In this method, the minimum norm vector is identified as a vector located within the noise subspace, with the first element set to '1' and having the smallest norm. According to the definition, this vector can be expressed as follows, [14]:

$$\mathbf{g} = \begin{bmatrix} 1 \\ \hat{\mathbf{g}} \end{bmatrix} \tag{17}$$

Identifying the Min-Norm vector allows for the determination of DOA angles based on the peak positions of the resulting power spectrum function.

$$P_{\min-norm}(\theta) = \frac{1}{\left| \mathbf{a}^H(\theta) \begin{bmatrix} 1 \\ \hat{\mathbf{g}} \end{bmatrix} \right|} \tag{18}$$

Future directions for this work could involve exploring additional aspects, such as DOA estimation with Minimum Redundancy Linear Arrays (MRLA) and DOA estimation with Time-Variant Amplitude (TVA), [19], [20].

## 4 Adaptive Beamforming in MU-MIMO

This section explores the analysis of the adaptive Beamforming (BF) algorithm, focusing on the concepts of Signal of Interest (SOI) and Signal Not of Interest (SNOI). This analysis is based on the schematic diagram models illustrated in Figure 2 (Appendix).

The Base Station (BS) is equipped with N Uniform Linear Array (ULA) antenna elements to accommodate multiple users simultaneously, while each mobile user is equipped with a single antenna element. Notably, BF algorithms can be implemented for a single user while treating signals from other users as sources of interference.

As shown in Figure 2 (Appendix), a scenario is presented where one user is assumed to be the only active user, serving as a reference for validating the BF process. Consequently, when multiple signal branches arrive at the BS, signal processing procedures are performed to direct the sum of all BS sensor input signals toward the specific direction of the SOI while suppressing interference sources by steering them toward the null direction of the SNOI.

Subsequently, the signals from the user at the BS can be combined at any given time, representing the complete received signal of the $k^{th}$ user within the Multi-User Multiple-Input Multiple-Output (MU-MIMO) system, [14]. The array factor of the elements can be expressed as:

$$\mathrm{AF}(\theta) = \sum_{n=1}^{N/2} w_n \cos\left[(2n-1)\varphi_n\right] \tag{19}$$

The output weight of the antenna element is defined as:

$$\varphi_n = \frac{\pi d}{\lambda}\sin\theta \tag{20}$$

In this context, d, λ, and θ represent the spacing between the elements of the antenna array, the wavelength of the signal, and the angle of the desired signal, respectively. For simplicity, let's assume that the Base Station (BS) is equipped with four antenna elements (N = 4). As a result, the total received output signal in the specified direction of interest, referred to as "SOI," is normalized to unity, indicating the normalized signal amplitude. This concept is detailed in Equation (21), [3].

$$y\left(\theta_{SOI}\right) = w_1 e^{\pm j(3/2)\varphi_1} + w_2 e^{\pm j(1/2)\varphi_2} + w_3 e^{\pm j(1/2)\varphi_1} + w_4 e^{\pm j(3/2)\varphi_2} = 1 \tag{21}$$

Likewise, in a scenario where three interference sources impact the desired signal, referred to as

"SOI," the directions of the output signals from the unwanted sources, known as SNOIs, are given in Equations (22), (23), and (24).

$$y\left(\theta_{SNOI_1}\right) = w_1 e^{\pm j(3/2)\varphi_1} + w_2 e^{\pm j(1/2)\varphi_2} + w_3 e^{\pm j(1/2)\varphi_1} + w_4 e^{\pm j(3/2)\varphi_2} \quad (22)$$

$$y\left(\theta_{SNOI_2}\right) = w_1 e^{\pm j(3/2)\varphi_1} + w_2 e^{\pm j(1/2)\varphi_2} + w_3 e^{\pm j(1/2)\varphi_1} + w_4 e^{\pm j(3/2)\varphi_2} \quad (23)$$

$$y\left(\theta_{SNOI_3}\right) = w_1 e^{\pm j(3/2)\varphi_1} + w_2 e^{\pm j(1/2)\varphi_2} + w_3 e^{\pm j(1/2)\varphi_1} + w_4 e^{\pm j(3/2)\varphi_2} \quad (24)$$

By examining Equations (22), (23), and (24) and focusing on the removal of interference sources, it is clear that nullifying SNOIs from three different angles is essential. As a result, the sum of all weighted incoming unwanted signals equals zero, as shown in Equation (25).

$$y\left(\theta_{SNOI_1}\right) = y\left(\theta_{SNOI_2}\right) = y\left(\theta_{SNOI_3}\right) = 0 \quad (25)$$

There are four linear equations with four unknown variables that represent the required weights to be calculated. Thus, determining the weight values can be achieved easily through the linear solution of the Eq. 21, Eq. 22, Eq. 23, and Eq. 24), classifying this adaptive Beamforming (BF) as a linear algorithm. In contrast, several nonlinear adaptive BF algorithms diverge from this approach by using nonlinear methods for weight calculations. Consequently, the general expression for nonlinear adaptive BF can be formulated as follows:

$$T\frac{dw_n}{dt} + w_n = G\left(p_n - x_n^*(t)\sum_{i=1}^{N-1} w_i x_i(t)\right) \quad (26)$$

In this context, $T$ represents the time constant of the smoothing filter, while $G$ signifies the amplifier gain. $x_n(t)$ denotes the input signal from the $n^{th}$ antenna element, and $p_n$ indicates the cross-correlation result between xxx and the output of the primary antenna channel, referred to as the reference signal. The equation presented in (26) can be reformulated in matrix representation as follows:

$$\left.\begin{array}{l} w = \mu R^{-1} p \\ p = w^H R w \end{array}\right\} \quad (27)$$

where **R**, **w**, **p**, $\mu$ represent the correlation matrix (covariance matrix), the weight vector, the power vector, and the step size value, respectively. Additionally, the second part of this paper discusses the LMS, RLS, and Constant Modulus Algorithm (CMA) in relation to their ability to steer the desired signals toward the main response angle while suppressing interference signals. Furthermore, the latter section of this document examines the LMS, RLS, and CMA regarding their effectiveness in directing the desired signals to the primary response angle and reducing interference signals.

## 4.1 Least Mean-Squares Algorithm (LMS)

In the LMS algorithm, the estimation of signal weight elements involves calculating the mean squares in conjunction with the current weight value, which depends on the previous value. As shown in Figure 2 (Appendix), the LMS algorithm requires a reference signal or training sequence, denoted as d(t), to compute the estimation error e(t). This error represents the variance between the reference signal and the incoming output signals, as illustrated in Eq. (28).

$$e(i) = d(i) - y(i) \quad (28)$$

When applying the gradient operator to a scalar quantity and taking the expectation of the squared errors, the result can be expressed as:

$$\nabla\left(E\left(e(i)^2\right)\right) = -e^*(i)\cdot \mathbf{x}(i) \quad (29)$$

Let $\mathbf{w}_i$ be the weight vector at sample time $i$; then the updated vector at time $i$+1 is represented as shown in Equation (30), [21].

$$\mathbf{w}(i+1) = \mathbf{w}(i) - \text{step}\cdot\nabla\left(E\left(e(i)^2\right)\right) \quad (30)$$

## 4.2 Recursive Least Squares (RLS)

The RLS algorithm utilizes the least-squares method to update weight elements by minimizing an exponentially weighted cost function. This cost function consists of two components: the sum of weighted squared errors and a regularization term. To simplify the representation, the weight updates can be expressed in matrix notation as outlined in reference, [22].

$$\mathbf{w}(i+1) = \mathbf{w}(i) + \frac{\mathbf{R}^{-1}(i)e^*(i+1)\mathbf{x}(i+1)}{\lambda + \mathbf{x}^H(i+1)\mathbf{R}^{-1}(i)\mathbf{x}(i+1)} \quad (31)$$

Importantly, the inverse of the newly updated inverse correlation matrix $\mathbf{R}^{-1}(i+1)$ can be expressed as follows:

$$\mathbf{R}^{-1}(i+1) = \frac{1}{\lambda}\left[\mathbf{R}^{-1}(i) - \frac{\mathbf{R}^{-1}(i)\mathbf{x}(i+1)\mathbf{x}^H(i+1)\mathbf{R}^{-1}(i)}{\lambda + \mathbf{x}^H(i+1)\mathbf{R}^{-1}(i)\mathbf{x}(i+1)}\right] \quad (32)$$

Here, λ represents a small positive forgetting constant factor, with a value less than one (λ < 1). The initial value of the correlation matrix is denoted by $\mathbf{R}^{-1}(0) = \delta^{-1}\mathbf{I}$, where δ is a positive constant that depends on the signal-to-noise ratio (SNR) level. In high SNR scenarios, the value of δ is small, while in low SNR situations, δ is larger. The matrix $\mathbf{I}$ represents the square $N \times N$ identity matrix. The revised $i^{th}$ correlation matrix can be expressed as:

$$\mathbf{R}^{-1}(i) = \mathbf{A}(i)\mathbf{A}^H(i) \quad (33)$$

And the matrix $\mathbf{A}$ can be given by:

$$\mathbf{A}(i+1) = \frac{1}{\sqrt{\lambda}}\left[\mathbf{A}(i) - \gamma\mathbf{A}(i)\mathbf{A}^H(i)\mathbf{x}(i)\mathbf{x}^H(i)\mathbf{A}(i)\right] \quad (34)$$

where $\mathbf{A}^{-1}(0) = \delta^{-1}\mathbf{I}$.

### 4.3 Constant Module Algorithm (CMA)

The CMA algorithm is utilized in communication channels that employ digital phase shift modulations such as PSK, BPSK, GMSK, and QPSK. As a result, the algorithm performs particularly well when signals have a consistent envelope.

Moreover, CMA beamforming is classified as a blind adaptive beamforming algorithm, allowing for weight updates without requiring any prior information about the desired signal. Additionally, the CMA technique takes advantage of the constant or nearly constant amplitude characteristics of most modulation techniques used in wireless networks. However, when the signal is received by the array, the receiver maintains a fixed amplitude, and the CMA updates the weights as follows: $w(n+1) = w(n) - \mu x(n)\varepsilon^*(n)$, where $\varepsilon^*(n) = \left[1 - |y(n)|^2\right] y(n)x(n)$, $\mu$ is a small step-size factor which is selected to guarantee the weight solution converges to the optimal minimum solution, [23], [24]. It is acknowledged that the updating of weight elements relies solely on the current value of the received signal. Therefore, the output signal of the CMA is expressed as:

$$y(i) = \mathbf{w}_{CMA}^H(i)\mathbf{x}(i) \quad (35)$$

The weight update in the CMA method resembles that of the LMS algorithm; however, the error is calculated based on the actual received signal. Therefore, the next weight update in the CMA technique is expressed as follows, [7], [25], [26]:

$$\mathbf{w}_{CMA}(i+1) = \mathbf{w}_{CMA}(i) - \mu\mathbf{x}(i)\left(|y(i)|^2 - 1\right)y^H(i) \quad (36)$$

The output signal of the antenna array sensor is generated by multiplying the weight vector with the input signals vector, as shown:

$$y = \mathbf{w}^H\mathbf{x} \quad (37)$$

However, the total average output power after applying the Beamforming (BF) algorithm can be calculated using the updated weights, [27], as outlined below:

$$P_T = E\{w^H x x^H w\} = w^H E\{x x^H w\} = w^H R\, w \quad (38)$$

where the channel correlation matrix $xx^H$ is $\mathbf{x}\mathbf{x}^H = \mathbf{R}$. The probability of achieving the minimum bit error rate (BER) $P_{BER}$ [28] can be derived as:

$$\begin{aligned} P_{BER}(e)_{\min} &= Q\left(\sqrt{\frac{P_T T_b}{N_o/2}}\right) = Q\left(\sqrt{\frac{E_b}{N_o/2}}\right) \\ &= Q\left(\sqrt{\frac{P_T}{R_b N_o/2}}\right) \end{aligned} \quad (39)$$

where $P_T$, $R_b$, and $T_b$ are the total average transmit signal power, the transmission channel bit rate, and the bit period, respectively.

## 5 Results and Discussion

In this section, the results achieved in this study will be presented and discussed.

### 5.1 The Power Spectrum

The results shown in Figure 3 illustrate a comparison of different Beamforming (BF) algorithms, including conventional BF, MUSIC, MVDR, and Min-Norm algorithms. These findings highlight the relationship between the Direction of Arrival (DOA) and the signal power spectrum. The expected arrival angles are assumed to [-π/3°, 0°, and π/4°], with the Base Station (BS) equipped with 32 antenna elements. Notably, the Angle of Arrival (AOA) for all DOA algorithms is quite similar.

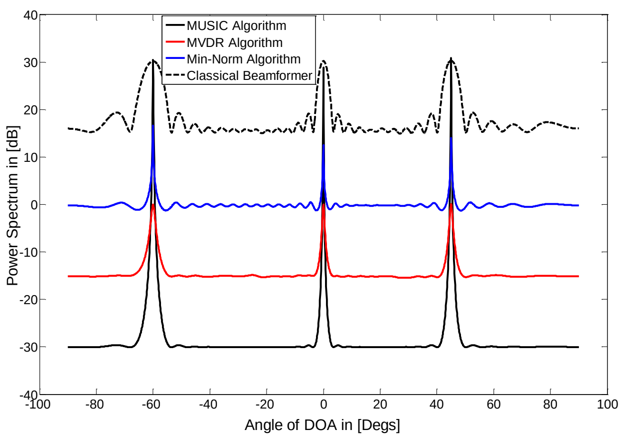


Fig. 3: The direction of arrival algorithms using 32 antennae (M=32)

Regarding beam width, the results indicate that the MVDR and Min-Norm methods produce a similar beam width, despite variations in the peak signal power spectrum values. Specifically, the MVDR achieves 0 dB while the Min-Norm reaches 15 dB. In contrast, the sidelobes of the MUSIC, MVDR, and Min-Norm algorithms are compared to the classical beamformer, which serves as a reference for traditional DOA algorithms, as shown in Figure 3 and Figure 4.

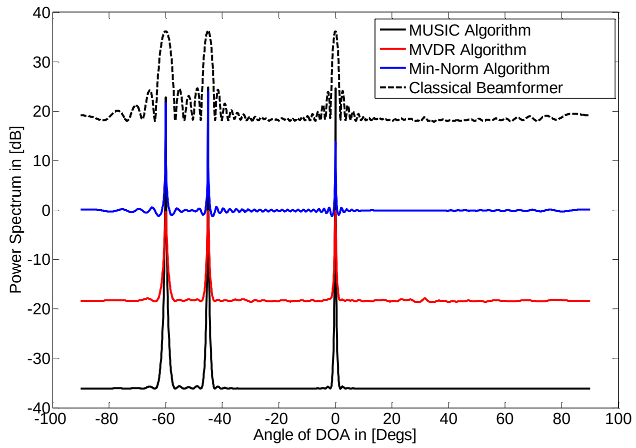


Fig. 4: The direction of arrival algorithms using 64 antennae (M=64)

Figure 4 illustrates the results obtained using 64 antennas with Angle of Arrival (AOA) angles of -π/3º, -π/4º, and 0º. The peak power notably increases to around 37.5 dB, with a significant reduction in sidelobes due to the array elements concentrating signal energy toward the main beam direction, thus enhancing directivity.

In Figure 5, results from 128 antennas with the same AOA angles demonstrate a complete minimization of insignificant sidelobes, along with a peak signal power increase to 43 dB. This suggests that the MUSIC algorithm exhibits greater sensitivity to weak incoming signals compared to other methods, while traditional techniques require stronger incoming signals for optimal performance.

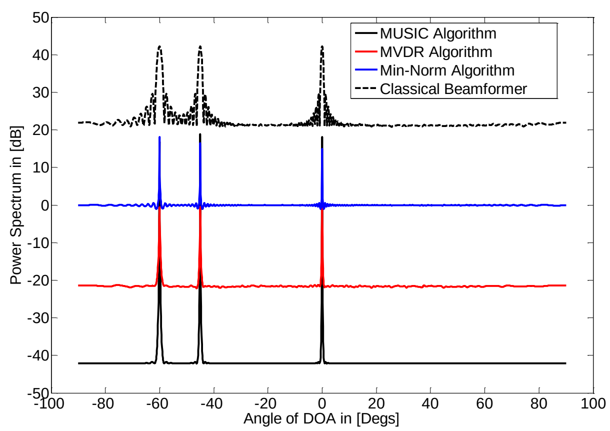


Fig. 5: The direction of arrival algorithms using 128 antennae (M=128)

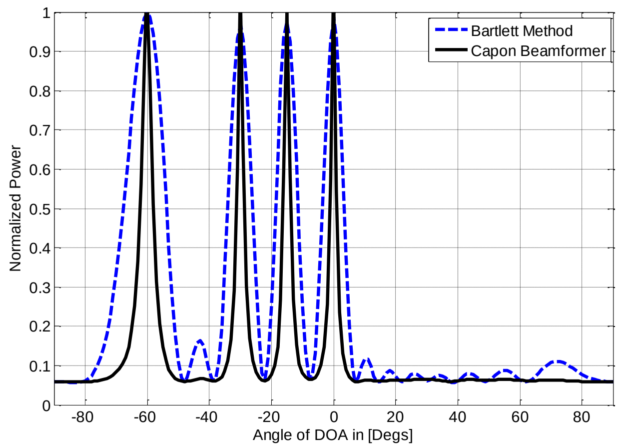


Fig. 6: Normalized power spectrum of Bartlett and Capon algorithms using 16 antennae (M=16)

The results shown in Figure 6 compare the Bartlett and Capon methods using 16 antenna elements with DOA angles of -60º, -30º, -15º, and 0º. Notably, the normalized power spectrum of both methods displays similar characteristics; however, the Capon method achieves near-null sidelobes and narrower beam width. Figure 7 presents results with 64 antennas, demonstrating significantly narrower beam angles in comparison to those in Figure 6. Overall, the findings indicate comparable performance and signal power response between the Bartlett and Capon methods.

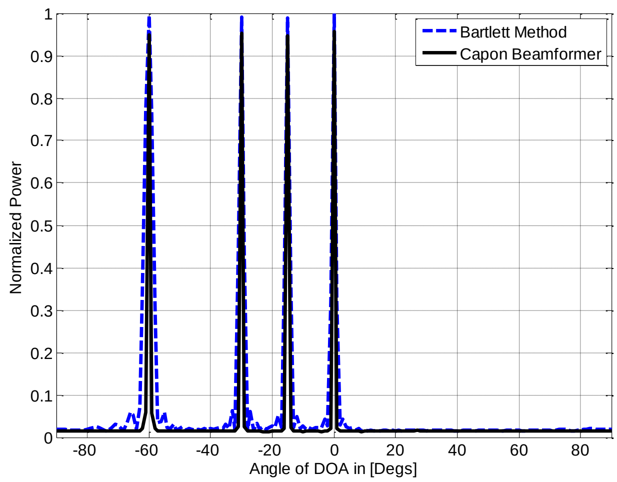


Fig. 7: Normalized power spectrum of Bartlett and Capon algorithms using 64 antenna (M=64)

## 5.2 The Amplitude Radiation

Figure 8 presents the beamforming results for the LMS, RLS, and CMA algorithms, showing the normalized signal amplitude in relation to the angle of arrival (AOA) with two antenna elements at the base station. The results indicate that the algorithms produce similar outcomes in terms of main beam gain (in the direction of the signal of interest). However, in the direction of interference suppression at at -10° AOA, the RLS algorithm significantly outperforms both the LMS and CMA, with an amplitude difference of nearly −20 dB. This enhancement is attributed to the RLS algorithm's use of least square error (LSE), which improves the accuracy of weight updates.

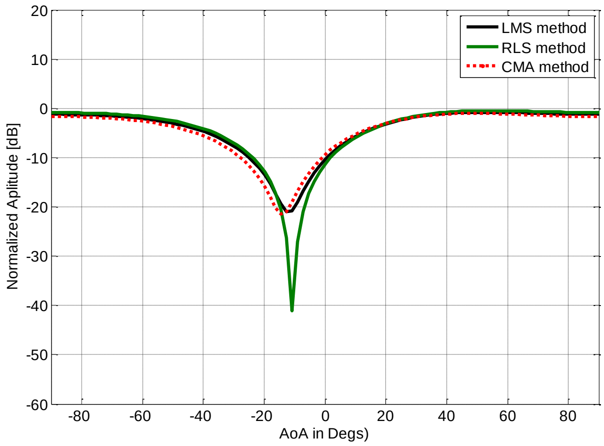


Fig. 8: Radiation magnitude versus AOA using two antennae at the BS

Similarly, Figure 9 displays the results of the beamforming algorithm using four antenna elements at the base station. Increasing the number of antenna elements enables the beamformer to more effectively suppress interference in a specific direction. The results indicate that the LMS and RLS algorithms perform comparably, achieving a magnitude of −50 dB, which suggests that effective nulls are created to reduce interference.

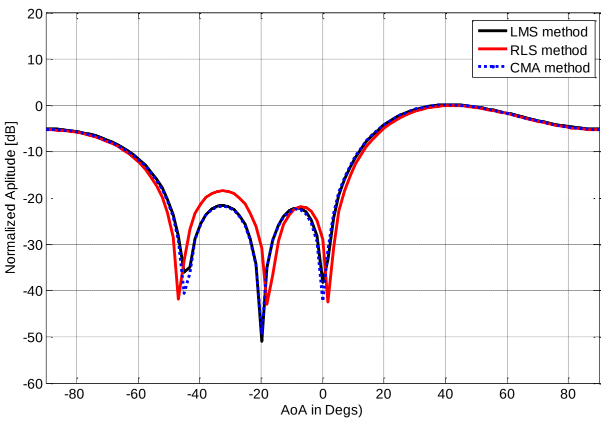


Fig. 9: Radiation magnitude versus AOA when using four antennae at the BS

Figure 10 illustrates the results for the algorithms with different numbers of base station antenna elements, specifically with eight elements deployed. It is clear that as the number of antenna elements increases, the RLS beamformer achieves interference attenuation of up to −58 dB at a specific angle (approximately 75°, where the corresponding normalized power is −58 dB). These findings demonstrate that as the number of base station antenna elements increases, the beamforming algorithms discussed in this paper can effectively cancel interference.

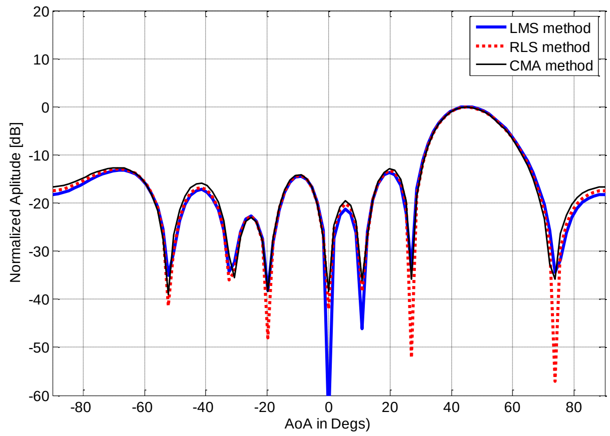


Fig. 10: Radiation magnitude versus AOA for beamforming algorithms using eight antennae at the BS

## 5.3 The Bit Error Rate

In this section, the performance metric Bit Error Rate (BER) is discussed in relation to the data rate and throughput of the system. BER is a crucial factor in evaluating beamforming performance.

Figure 11 presents the BER results for the MU-MIMO system using two antennas (M=2) at the base station. At a BER = $10^{-3}$ the $E_b/N_o$ = 30 dB for the system without beamforming and 16 dB for the system with beamforming. These results indicate that the BER performance with beamforming is significantly better than that without it.

Figure 12 illustrates the BER results in relation to the number of antennas (M = 4) at the base station. It is observed that to achieve a specific BER i.e. BER = $10^{-3}$ the $E_b/N_o$ = 30 dB for the considered system without BF and $E_b/N_o$ = 8 dB for the considered system with BF.

Figure 13 presents the BER results for the system using eight antennas (M=8) at the base station, at BER = $10^{-3}$ the $E_b/N_o$ = 30 dB for the considered system without BF and $E_b/N_o$ = 4 dB for the considered system with BF, again showing improved performance with BF compared to without it. It is evident that increasing the number of antenna elements significantly enhances the BER results.

Adam Mohamed Ahmed Abdo,
Mohamed Hussien Mohamed Nerma,
Aamer Mohamed Huroon Mohamed

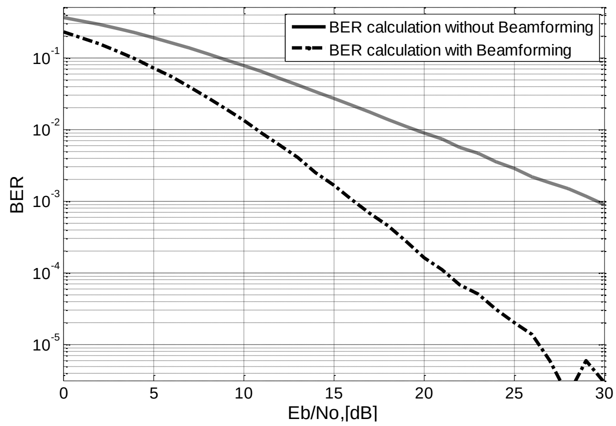

Fig. 11: The BER using two antennae at the BS

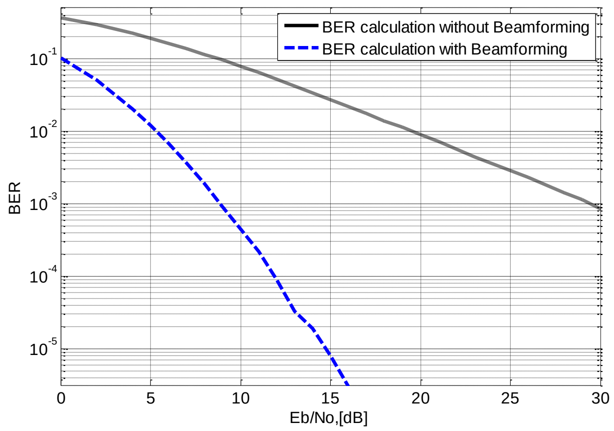

Fig. 12: The BER using four antennae at the BS

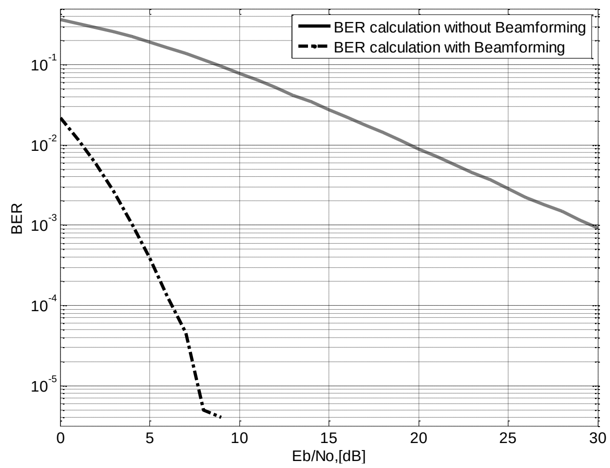

Fig. 13: The BER using eight antennae at the BS

# 6 Conclusion and Future Work

In this paper, various beamforming (BF) algorithms for Direction of Arrival (DOA) estimation were investigated and analyzed. The simulation results were conducted regarding scanning angles and peak power spectrum. The findings indicated that the choice of an appropriate DOA technique depends on the balance between peak signal power, interference suppression, and beam width.

Various nonlinear adaptive beamforming algorithms and their Bit Error Rate (BER) performance for MU-MIMO communication systems were examined and analyzed. The SMI, RLS, and CMA beamforming algorithms were thoroughly examined in terms of managing data signals and interference sources. It was confirmed that the efficiency of these algorithms improves with an increased number of antenna elements at the base station.

For the BER results, at a BER of $10^{-3}$, the system using two antennas with beamforming achieved an $E_b/N_o$ of 16 dB, while the system without beamforming achieved 30 dB. With four antennas, the system implementing beamforming yielded an $E_b/N_o$ of 8 dB, whereas the system without beamforming provided 30 dB. When using eight antennas, the beamforming system reached 4 dB of $E_b/N_o$, in contrast to 30 dB for the system without beamforming. Means, the BER significantly improves when beamforming is implemented.

Finally, this research can be further extended to future networks to address the rapid advancements in wireless cellular mobile communications. It can also be enhanced to accommodate massive MU-MIMO antenna elements suitable for higher millimeter-wave frequency bands, thus meeting the requirements of beyond sixth-generation (6G) networks. Consequently, artificial intelligence (AI) techniques may be integrated with advanced signal processing and adaptive DOA methods. This integration is expected to yield significant new results, with a focus on adaptive scaling of user signals and dynamic adjustment of beamforming weights. Additionally, considering the two-dimensional array elements (UPA) promises to provide more accurate DOA angle estimations.

**Declaration of Generative AI and AI-assisted Technologies in the Writing Process**

During the preparation of this work, the authors used GPT-3.5-Turbo to improve the writing process. After using this tool/service, the authors reviewed and edited the content as needed and take full responsibility for the content of the publication.

*References:*

[1] K. Wei, J. Xu, W. Xu, N. Wang and D. Chen, "Distributed Neural Precoding for Hybrid mmWave MIMO Communications With Limited Feedback," in *IEEE*

*Communications Letters*, vol. 26, no. 7, pp. 1568-1572, July 2022, doi: 10.1109/LCOMM.2022.3167712.

[2] A. M. A. Abdo, A. M. H. Mohamed, M. A. S. Ali, M. E. A. Adam and X. Zhao, "Nonlinear Adaptive Beamforming Algorithms and Bit Error Rate Analysis for MU MIMO m mWave Communication System," *2019 International Conference on Computer, Control, Electrical, and Electronics Engineering (ICCCEEE)*, Khartoum, Sudan, 2019, pp. 1-6, doi: 10.1109/ICCCEEE46830.2019.9071350.

[3] F. Rashid-Farrokhi, K. R. Liu, and L. Tassiulas, "Transmit beamforming and power control for cellular wireless systems," *IEEE Journal on Selected Areas in Communications*, vol. 16, no. 8, pp. 1437-1450, Oct. 1998, doi: 10.1109/49.730452.

[4] L. Yang, M. R. McKay and R. Couillet, "High-Dimensional MVDR Beamforming: Optimized Solutions Based on Spiked Random Matrix Models," in *IEEE Transactions on Signal Processing*, vol. 66, no. 7, pp. 1933-1947, 1 Aprill, 2018, doi: 10.1109/TSP.2018.2799183.

[5] D. N. Patel, B. J. Makwana and P. B. Parmar, "Comparative analysis of adaptive beamforming algorithm LMS, SMI and RLS for ULA smart antenna," *2016 International Conference on Communication and Signal Processing (ICCSP)*, Melmaruvathur, India, 2016, pp. 1029-1033, doi: 10.1109/ICCSP.2016.7754305.

[6] Amara Prakasa Rao, N. V. S. N. Sarma, "Adaptive Beamforming Algorithms for Smart Antenna Systems," *WSEAS Transactions on Communications*, vol. 13, pp. 44-50, 2014, [Online]. https://wseas.com/journals/articles.php?id=4714 (Accessed Date: October 28, 2024).

[7] P. Chevalier, J. -P. Delmas and M. Sadok, "Third-Order Volterra MVDR Beamforming for Non-Gaussian and Potentially Non-Circular Interference Cancellation," in *IEEE Transactions on Signal Processing*, vol. 66, no. 18, pp. 4766-4781, 15 Sept.15, 2018, doi: 10.1109/TSP.2018.2860551.

[8] X. Zhang, X. Liu, H. Yu, and C. Liu, "Improved MUSIC algorithm for DOA estimation of coherent signals via toeplitz and fourth-order-cumulants," *International Journal of Control and Automation*, vol. 8, No. 10, pp. 261-272, 2015, doi:10.14257/ijca.2015.8.10.25.

[9] S. Bhuiya, F. Islam, and M. Matin, "Analysis of direction of arrival techniques using uniform linear array," *International Journal of Computer Theory and Engineering*, vol. 4, No. 6, pp. 931-934, 2012, doi:10.7763/IJCTE.2012.V4.609.

[10] Y. Khmou, S. Safi, and M. Frikel, "Comparative study between several direction of arrival estimation methods," *Journal of Telecommunications and Information Technology*, No. 1, pp. 41-48. 2014, doi:10.26636/jtit.2014.1.1004.

[11] E. Gentilho Jr, P. R. Scalassara, and T. Abrão, "Direction-of-arrival estimation methods: A performance-complexity tradeoff perspective," *Journal of Signal Processing Systems,* vol. 92, pp. 239-256, 2020, doi.org/10.1007/s11265-019-01467-4.

[12] X. Zhao, A. M. A. Abdo, C. Xu, S. Geng, J. Zhang and I. Memon, "Dimension Reduction of Channel Correlation Matrix Using CUR-Decomposition Technique for 3-D Massive Antenna System," in *IEEE Access*, vol. 6, pp. 3031-3039, 2018, doi: 10.1109/ACCESS.2017.2786681.

[13] L. Zhao, D. W. K. Ng and J. Yuan, "Multi-User Precoding and Channel Estimation for Hybrid Millimeter Wave Systems," in *IEEE Journal on Selected Areas in Communications*, vol. 35, no. 7, pp. 1576-1590, July 2017, doi: 10.1109/JSAC.2017.2699378.

[14] J. Foutz, A. Spanias, and M. K. Banavar, Narrowband direction of arrival estimation for antenna arrays, *Synthesis Lectures on Antennas,* Springer Cham Publisher, 2008, doi.org/10.1007/978-3-031-01537-3.

[15] M. U. Rahman, "Performance analysis of MUSIC DOA algorithm estimation in multipath environment for automotive radars," *International Journal of Applied Science and Engineering*, vol. 14, No. 2, pp. 125-132, 2016, doi.org/10.6703/IJASE.2016.14(2).125.

[16] J. Ma, M. Wang, Y. Chen and H. Wang, "Deep Convolutional Network-Assisted Multiple Direction-of-Arrival Estimation," in *IEEE Signal Processing Letters,* vol. 31, pp. 576-580, 2024, doi: 10.1109/LSP.2024.3359888.

[17] R. Kerstens, T. Verellen, and J. Steckel, "Comparing adaptations of MUSIC beamforming for 3D in-air sonar applications with coherent source-spaces," in *8th Berlin Beamforming Conference* 2020, pp. 1-12,

2020, https://hdl.handle.net/10067/1664480151162165141 (Accessed Date: October 28, 2024).

[18] K. H. Lee, "A Study on the Desired Target Signal Estimation using MUSIC and LCMV Beamforming Algorithm in Wireless Coherent Channel," *International journal of advanced smart convergence*, vol. 9, No. 1, pp. 177-184, 2020, doi: 10.7236/IJASC.2020.9.1.177.

[19] Xiaoli Ren, Ji Wang, Shuangyin Liu, "A Sparse Signal Reconstruction Perspective for Direction-of-Arrival Estimation with Minimum Redundancy Linear Array," *WSEAS Transactions on Signal Processing*, vol. 10, pp. 374-381, 2014, [Online]. https://wseas.com/journals/articles.php?id=5201 (Accessed Date: October 28, 2024).

[20] Habti Abeida, "Direction-of-Arrival Estimation of a Single Distorted Wavefront with Time-Variant Amplitude," WSEAS Transactions on Signal Processing, vol. 12, pp. 16-27, 2016, [Online]. https://wseas.com/journals/articles.php?id=3755 (Accessed Date: October 28, 2024).

[21] C. Sun and J. Ding, "Application of the DOA Algorithms in the Uniform Circular Array Antennas," *2018 International Conference on Intelligent Transportation, Big Data & Smart City (ICITBS)*, Xiamen, China, 2018, pp. 633-636, doi: 10.1109/ICITBS.2018.00165.

[22] I. Uchendu and J. R. Kelly, "Survey of beam steering techniques available for millimeter wave applications," *Progress In Electromagnetics Research*, vol. 68, pp. 35-54, 2016, doi: 10.2528/PIERB16030703.

[23] C. A. Pitz, E. L. O. Batista and R. Seara, "On the Joint Beamforming and Power Control in Cellular Systems: Algorithm and Stochastic Model," in *IEEE Transactions on Wireless Communications*, vol. 13, no. 12, pp. 6943-6954, Dec. 2014, doi: 10.1109/TWC.2014.2359021.

[24] D. Godard, D. Godard, "Self-Recovering Equalization and Carrier Tracking in Two-Dimensional Data Communication Systems," in *IEEE Transactions on Communications*, vol. 28, no. 11, pp. 1867-1875, November 1980, doi: 10.1109/TCOM.1980.1094608.

[25] J. Treichler and B. Agee, "A new approach to multipath correction of constant modulus signals," in *IEEE Transactions on Acoustics, Speech, and Signal Processing*, vol. 31, no. 2, pp. 459-472, April 1983, doi: 10.1109/TASSP.1983.1164062.

[26] I. Irfanullah, "Adaptive Beamforming for Antennas on General Wedge-and Cylindrical-Shaped Surfaces," North Dakota State University, Ph.D. Dissertation, 2013, [Online]. https://hdl.handle.net/10365/27051 (Accessed Date: October 28, 2024).

[27] H. B. Kassa, T. Y. Chernet, E. Yohannes, D. Hailemariam, Y. Astatke, and F. Moazzami "Investigation of RLS beamforming algorithm interms of energy efficiency," *2016 Annual Conference on Information Science and Systems (CISS)*, Princeton, NJ, USA, 2016, pp. 82-86, doi: 10.1109/CISS.2016.7460481.

[28] A. A. M. Khalaf, A. -R. B. M. El-Daly and H. F. A. Hamed, "Different adaptive beamforming algorithms for performance investigation of smart antenna system," *2016 24th International Conference on Software, Telecommunications and Computer Networks (SoftCOM)*, Split, Croatia, 2016, pp. 1-6, doi: 10.1109/SOFTCOM.2016.7772134.

## Contribution of Individual Authors to the Creation of a Scientific Article (Ghostwriting Policy)

The authors equally contributed in the present research, at all stages from the formulation of the problem to the final findings and solution.

## Sources of Funding for Research Presented in a Scientific Article or Scientific Article Itself

No funding was received for conducting this study.

## Conflict of Interest

The authors have no conflicts of interest to declare.

# APPENDIX

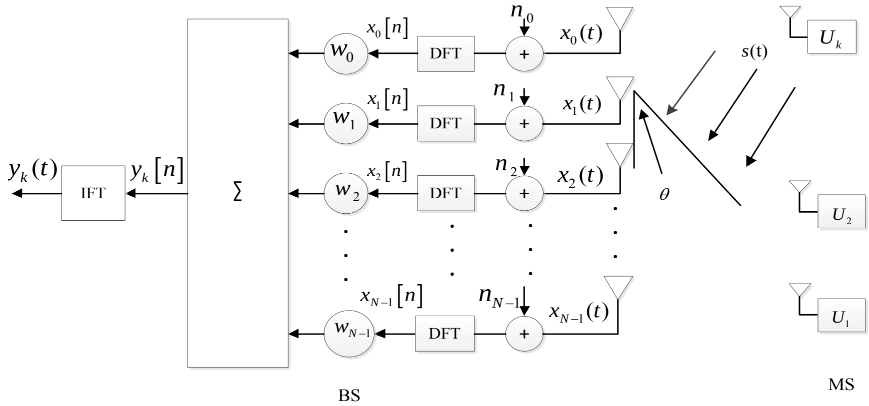


Fig. 1: The direction of arrival estimation

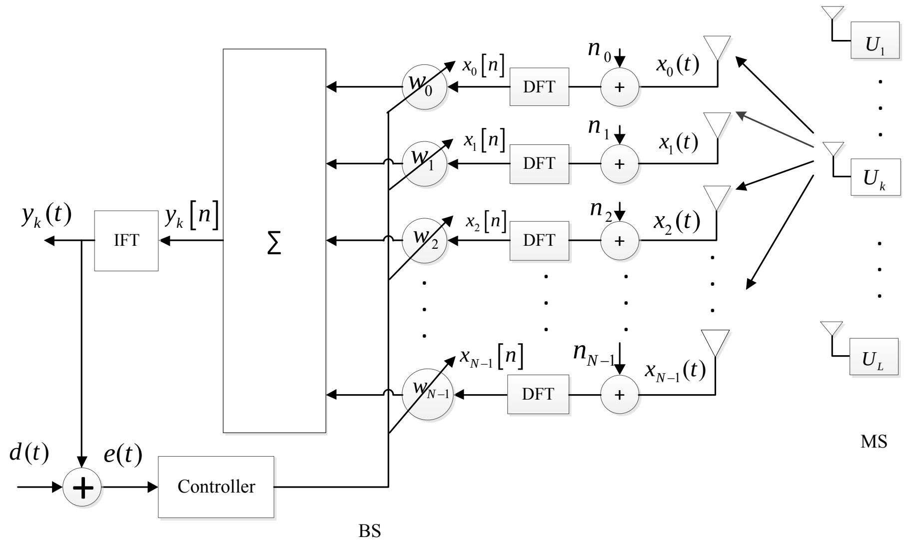


Fig. 2: The adaptive beamformer designed for a uniform linear array antenna within the context of the MU-MIMO system